

## ENERGY BASED EVALUATION OF GAS COOLING RELATED TO ARC FAULTS IN MEDIUM VOLTAGE SWITCHGEAR

Thomas Oyvang  
Telemark University College (TUC) – Norway  
[thomas.oyvang@hit.no](mailto:thomas.oyvang@hit.no)

Wilhelm RONDEEL  
TUC – Norway  
[wilhelm.rondeel@hit.no](mailto:wilhelm.rondeel@hit.no)

Elin FJELD  
TUC – Norway  
[elin.fjeld@hit.no](mailto:elin.fjeld@hit.no)

Svein Thore Hagen  
TUC – Norway  
[svein.t.hagen@hit.no](mailto:svein.t.hagen@hit.no)

Knut VAAGSAETER  
TUC – Norway  
[knut.vagsather@hit.no](mailto:knut.vagsather@hit.no)

### ABSTRACT

*An arc fault inside metal enclosed switchgear causes a rise in gas temperature and pressure and may endanger the safety of personnel. Passive devices that effectively cool down the gas with limited extra cost are of special interest to investigate. An energy based evaluation of different gas cooling installations and materials related to internal arc faults in medium voltage switchgear has been carried out. Temperature measurement in inhomogeneous gas flows constitutes a central part of this study. A thermal efficiency of 79 % ( $\Delta T$  of 540 K) is observed with an aluminium mesh as absorption material. The energy distribution in the system is visualized in a Sankey diagram showing that 2/3 of the energy is absorbed in the arc compartment. The remaining energy enters a buffer room, from which about 50 % escapes through an energy absorber. Depending on design, between 5 and 10 % of the total energy input from the electric arc escapes to the surroundings. By introducing boric acid in the absorber, cooling by ablation seemed to take place. Depending on buffer and absorber design, the observed pressure rises in the arc compartment indicate that some precautions may have to be taken to avoid excessive stress on the switchgear compartment (arc compartment). Based on the experimental setup presented in this paper, 5 of 6 tests with different designs passed the standard safety test.*

### INTRODUCTION

The continuing development of modern switchgear, combined with dedicated testing based on international standards and in particular the IEC 62271-200 standard [1], has significantly increased the safety of switchgear. Overpressure may be controlled by relief openings guiding hot gases away from personnel. In some installations exhaust gas may need to be cooled to avoid hazard of injury. Earlier works [2, 3] show that arc energy absorbers in electrical installations may reduce external overpressure and temperature by heat absorption and flow resistance.

This investigation presents an evaluation of different gas cooling installations and materials in connection with internal arc faults in medium voltage switchgear. The

evaluation is based on heat transfer, energy balance and temperature/pressure measurements. Some energy absorption materials with designs that may effectively cool the exhaust gas are tested and evaluated. Expanded aluminium and steel are used as base materials. In addition boric acid ( $H_3BO_3$ ) and paraffin wax are introduced, intending to utilize phase shift energy absorption by melting and/or ablation as these processes dissipates relatively large quantities of energy. Utilisation of boric acid is well known as an arc quenching material in expulsion fuses for high power applications. Based on the test results, temperature, pressure, the thermal efficiency, absorbed heat, energy balance, and absorber designs are determined and evaluated.

### TEST OBJECTS AND EXPERIMENTAL SETUP

The evaluation is based on internal arc experiments in air within an arc compartment (A) as shown in Figure 1 with two pressure relief openings. Overpressure is relieved into a semi-enclosed buffer room (B). The relief opening of the buffer room is equipped with a cooling system to absorb energy from the exhaust gas (C). The exhaust gas and associated energy flow from the arc compartment through the absorber is monitored with pressure sensors ( $P_1$  to  $P_2$ ) shown in Figure 2, different types of thermocouples ( $T_1$  to  $T_{10}$ ), surface measurements ( $T_{11}$  and  $T_{12}$ ), and by studying high speed videos. Temperatures were measured with thermocouples and CelsiStrip outside on A and B as shown in Table 1.

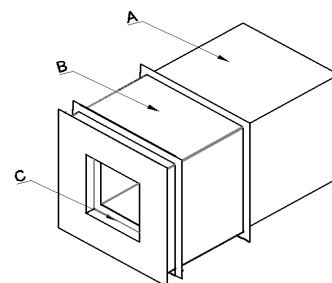


Figure 1. Test arrangement made of steel existing of arc compartment (A) with volume  $0.343 \text{ m}^3$  with two pressure relief openings of 110 mm in diameter. Exhaust gas is relieved into a semi-enclosed buffer room (B) with volume of  $0.245 \text{ m}^3$ . The relief opening of the buffer room is equipped with a cooling system (C) with a volume of  $0.0235 \text{ m}^3$  to absorb energy from the exhaust gas.

All experiments were performed at NEFI High Power Laboratory in Skien, Norway. A total of 6 experiments were carried out with Cu electrodes of 20 mm in diameter in a single phase arrangement in enclosure A with arc duration of 1.0 second. The gap distance between the electrodes was initially 100 mm. The test current was 15.5 kA<sub>rms</sub> AC, (50 Hz) with a supply voltage of 4.76 kV, an asymmetric peak factor of 2.3, and a typical arc voltage of 290 V. The relatively high supply voltage, combined with a power factor less than 0.17, secured reignition at each current zero. In all the experiments arc voltage, current, temperature, and pressure were recorded by the metering system of the laboratory.

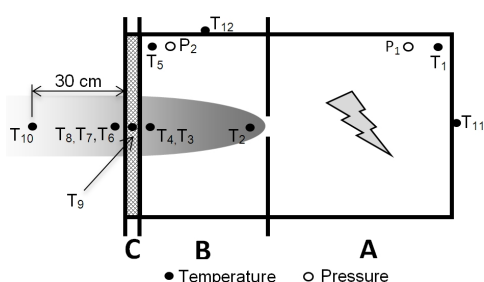


Figure 2. Cross section sketch (sideview) of test arrangement showing location of the sensors. Pressure sensors P<sub>1</sub> and P<sub>2</sub>, thermocouples T<sub>1</sub> to T<sub>10</sub> and temperature surface measurement T<sub>11</sub> and T<sub>12</sub>.

Table 1 Temperature measurements

Thermocouples	Element	Probe diameter
T <sub>1</sub> - T <sub>7</sub> , T <sub>9</sub> , T <sub>10</sub>	K	0.5 mm
T <sub>8</sub>	K	0.015 mm
T <sub>11</sub> , T <sub>12</sub>	CelSiStrip	-

The details of the cooling system, also called absorber (C), in the different tests are shown in Table 2. Test 1 was carried out with enclosure (A) only, with its two pressure relief openings. This test is the reference test for the pressure and temperature inside the arc compartment without buffer and absorber. The absorber unit chassis (shown in Figure 3) is made of 3 mm steel and has a cross flow area of 0.15 m<sup>2</sup> and a weight of 8.2 kg.

Table 2 Experimental conditions of the cooling system (C)

Test no	Material	No of Layers	Absorber medium and unit design	Fig. 3
1	Reference test without absorber and buffer (only A in Figure 1)			
2	Aluminium Expanded mesh Calendered, Diamond	5	Spacer between layers Size: (20x10-1,5x1,5) Weight of Al: 1.2 kg	Left
3	Galvanized Steel Expanded mesh Calendered, Diamond	4	Size: (20x10-1,5x1,5) Weight of Steel: 3.01 kg	Right
4	Aluminium Expanded mesh Flattened, Square	10	Roll Size: (3x2,2-0,3x0,4) Weight of Al: 1.2 kg	Middle
5	See test 2 Paraffin wax Flash point: 150 C°	5	Weight of Al: 1.2 kg Paraffin wax: 2 kg	Left
6	Galvanized Steel Expanded mesh Calendered, Diamond	4	Size: (20x10-1,5x1,5) Weight of Steel: 3.01 kg Boric Acid H <sub>3</sub> BO <sub>3</sub> : 650g	Right



Figure 3. Left: Front view of absorber with expanded metal of aluminium for test 2. Middle: Open absorber showing an arrangement of rolls (with 10 layers) of expanded metal in test 4. Right: Open absorber showing an arrangement of expanded steel mesh with boric acid tablets in test 6.

### TEST RESULTS

Table 3 shows the average temperatures in Kelvin measured in test 2, 3, 4, and 6 with absorber. The average value is taken in the interval from 0.8 to 1.3 seconds after the initiation of the arc. The arc duration was 1 s, but the temperatures are quite stable in the first 0.3 s after the arc current has been switched off. The average values shown in Table 3 are therefore near the temperatures in the moment when the arc current is switched off.

Table 3 Average temperature from 0.8 to 1.3 seconds

Thermocouples	Location	Temperature, T[K]			
		Test no.			
		2	3	4	6
T <sub>3</sub> and T <sub>4</sub>	Before absorber	933	1073	963	1033
T <sub>6</sub> and T <sub>7</sub>	After absorber	451	581	423	518
T <sub>10</sub>	Indicators	430	445	354	387
T <sub>5</sub>	Buffer room	473			
T <sub>1</sub>	Arc compartment	1337			
T <sub>11</sub>	Surface arc compart.	346			
T <sub>12</sub>	Surface buffer room	< 313			

The thermal efficiency,  $\eta_T$ , of the absorber, is determined from [2]:

$$\eta_T = (\Delta T_{before} - \Delta T_{after}) / \Delta T_{before} \quad (1)$$

Here  $\Delta T_{before}$  and  $\Delta T_{after}$  are the recorded maximum gas temperature rises in front of and behind the absorber. Test 4 with aluminum rolls has the highest thermal efficiency of 79 % as shown in Table 4. Ambient temperature during the tests was 283 K.

Table 4 Thermal efficiency and temperature difference

	Test no.			
	2. Al	3. Steel	4. Al rolls	6. Boric Acid
$\eta_T$	0.74	0.62	0.79	0.69
( $\Delta T_{before} - \Delta T_{after}$ ) [K]	482	492	540	515

The paraffin wax in test 5 ignited and the temperature recordings were uncertain. Indicators (IEC test "cloth") located 30 cm from the absorber outlet were unharmed during all tests, except during this test (no 5). The thermocouples of T<sub>2</sub> went out of range immediately after the rupture of relief openings in all tests. T<sub>9</sub> located inside the absorber showed a slightly lower temperature compared to the temperature measurements before the absorber. However, the exact location of thermocouple T<sub>9</sub> varied with different types of absorbers and did not provide fully comparable values. The thermocouple T<sub>8</sub> with a smaller probe diameter, with a fast response time was used in test 2

and 3 only. A higher measured temperature compared to the other types of thermocouples at the same location was observed. Consequently temperature measurements should therefore, to some extent, be interpreted with some care. The lowest temperature measured after the absorber was in test 4 with aluminium rolls as shown in Table 3. The temperature before the absorber varied from 933 to 1073 K. In test 6 about 100 g boric acid disappeared and a lower exit temperature than in test 3 (same set-up except for the boric acid tablets) was recorded. In this test only one of the relief discs opened. There was no significant difference in maximum temperature inside arc compartment,  $T_1$ , with and without buffer/absorber as shown in Figure 4.

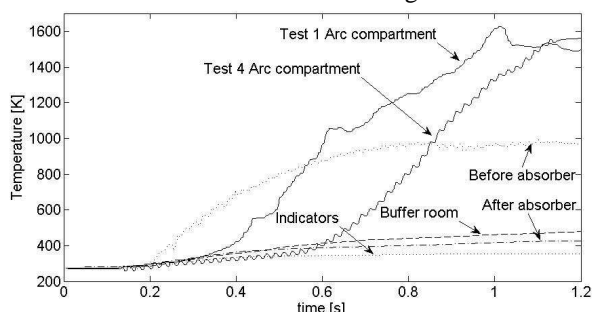


Figure 4 Temperature rise during test 4 for arc compartment ( $T_1$ ), before ( $T_4$ ) and after ( $T_7$ ) absorber, indicators 30 cm from outlet, ( $T_{10}$ ) and buffer room ( $T_3$ ). The temperature rise in the arc compartment in test 1 is included.

The pressure relief discs opened after 0.05 s, and released an ionized gas jet into the buffer room. Figure 5 shows the unrestricted gas jet in test 1. In test 4 the absorber has a relatively dense mesh design, and the gas flow through the absorber was more restricted than in the other tests. Part of the aluminium in the absorber melted, is shown in Figure 5.



Figure 5 Above: Melted aluminum on expanded mesh of steel from test 4. Below: Hot gas jet with length of 450 mm escaping through relief openings from arc compartment in test 1 without buffer, high speed camera exposure.

The measured maximum relative pressure in test 1 to test 5 for both arc compartment and buffer room is shown in Table 5 below.

Table 5 Measured maximum relative pressure

Pressure [bar]	location	Test no.					
		1	2	3	4	5	6
$\Delta p_1$	Arc compart.	1.68	1.71	1.76	1.9	1.66	-*
$\Delta p_2$	Buffer room	-	0.14	0.11	0.36	0.8	-*

\*Because of technical problems with the monitoring equipment, test results were lost during experiments.

In test 4 a higher relative pressure was recorded in both rooms compared to test 2 and 3. The pressure in the arc compartment and the buffer room for test 4 is shown in

Figure 6 together with the pressure in the arc compartment without buffer (Test 1).

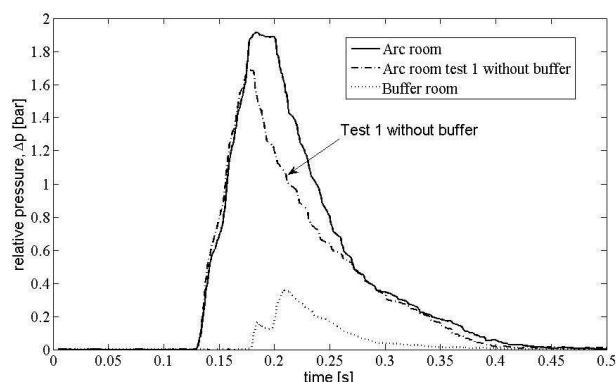


Figure 6 Measured relative pressure history in test 4 in arc compartment,  $p_1$ , and buffer room,  $p_2$  compared with pressure inside arc compartment for test 1 without buffer and absorber. The pressure fluctuation in the buffer room is caused by the different opening time of the two rupture discs in test 4.

## DISCUSSION

In general it was observed that the temperature recordings show significant variations depending on location, model and design of the thermocouples. Variation by location may explain the fact that the temperature in front of the absorber ( $T_4$ ) initially is higher than in the arc compartment ( $T_1$ ) from which the hot gases are ejected, Figure 4. It is furthermore observed that the registered temperatures before the absorber are influenced by the absorber design. In test 3 the flow restriction is relatively modest, and the plasma jet observed probably strikes the thermocouples quite directly due to a higher flow rate through the absorber design, see Figure 5. The direct flow may cause less mixing between the (original) air in the buffer room and the hot gas ejected from the arc compartment, resulting in a higher temperature recording in front of the absorber compared to the tests with a more restricted absorber flow.

As expected the pressure rise inside both arc and buffer room increases, maximum values shown in Table 5, as the absorber flow becomes more restricted. Only one rupture disc opened in test 5 and 6. In these tests the gas flow was restricted both by a reduced flow area and by the evaporation of paraffin wax and boric acid tablets, causing a counter pressure.

In test 4 to 6 energy absorption by melting and/or ablation of aluminium, paraffin, and boric acid was observed. Especially the introducing of boric acid seem to have increased the thermal efficiency of the absorber. The solid state boric acid applied in the experiments was shaped as "tablets", with a weight of 1 gram, diameter 16 mm, and 4 mm thick. Subjected to high temperatures boric acid will release water vapour, and by assuming a process comparable with the evaporation of water, 300 kJ may have been dissipated in test 6. Light gray steam is observed in the

video recordings.

In order to illustrate the final distribution of the energy dissipated a so-called Sankey diagram is drawn for test 4, Figure 7. The diagram is based on total arc energy and accumulated energy after 1 second, approximately 4500 kJ. The thermal transfer coefficient or "k<sub>p</sub>-factor", defined as the fraction of arc energy causing the pressure rise (until disc rupture), was 0.44. Energy required for heating, melting, and vaporizing the electrodes, "electrode arrangement", in Figure 7, is based on Oyvang et al. [4]. The maximum temperature recorded at the surface of the arc compartment (T<sub>11</sub>) was about 373 K. Assuming that effectively about 75 % of the total mass of the 100 kg arc compartment is heated to this temperature, the energy required is about 3000 kJ, or approximately 2/3 of the total energy input. The energy flow from the arc compartment into the buffer room depends on a number of factors, such as gas density, speed of sound, and specific heat. Some preliminary CFD simulations of the gas flow, based on ideal gas equations, delivered energy transport values too low to fit with our observations. The high speed exposures indicate gas temperatures in excess of those necessary for dissociation and ionization, Figure 5, and the specific heat of the gas ejected may be very high. Assuming that a 10 % fraction of the gas released into the buffer room is dissociated, the accumulated energy flow is approximately 1400 kJ. The energy required to increase the temperature of the buffer room structure by 30 K is estimated to about 700 kJ. If the assumption of 1400 kJ entering the buffer room is correct, about 50 % of the energy released into the buffer room is should then be entering the absorber. Based on observations of temperatures measured before, inside and after the absorber, also including the energy required (300kJ) for evaporation of boric acid (Test 6), we may conclude that at least 50 % of the energy leaving the buffer room is absorbed in the absorber.

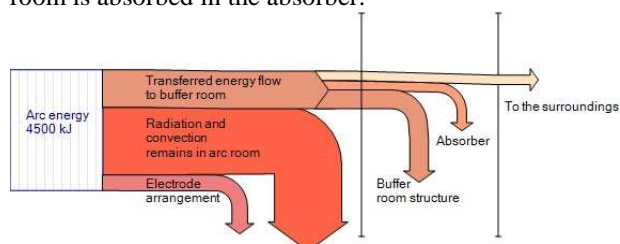


Figure 7 Sankey diagram indicating the energy distribution in the system.

The introduction of the buffer and absorber results in an increased maximum pressure in the arc compartment. The pressure in the arc compartment is increased during a period of about 0.1 s after the maximum pressure occurs. The consequence is an increased mechanical stress on the arc compartment. The recorded increase is not in a range that will result in the need of significant and expensive redesigns of switchgear where this type of buffer room and absorber may be applied.

The flow restriction and the gas cooling resulting from the

introduction of a buffer room with integrated energy absorber outlet causes a substantial reduction in the intensity of the energy release to the surroundings and hereby an increased personal safety is obtained.

## CONCLUSION

Based on temperature measurements the distribution of the accumulated energy input during an arc fault test has been estimated. The distribution of energy is visualized in a Sankey diagram, showing that approximately 2/3 of the energy input is absorbed in the arcing compartment. 50 % of the energy entering the buffer room is dissipated in the buffer room structure. At least 50 % of the energy leaving the buffer room is absorbed in the absorber. A thermal efficiency of 79 % and a  $\Delta T$  of 540 K are obtained with finely meshed aluminum as absorption material. In addition to a substantial cooling effect, the absorber contributes as a flow restriction, resulting in a more diffuse gas flow being expelled to the surroundings and to an improved safety for personnel. Testing proved that 5 of the 6 designs passed the standard safety test.

The maximum pressures recorded in these tests depend on the buffer and absorber design, but seem to be in a range that most probably will not result in the need of significant and expensive redesigns of relevant switchgear compartments. The introduction of the buffer and absorber results in an increased maximum pressure rise from 1.7 to 1.9 bar. The introduction of suitable materials to utilize phase shift energy absorption by melting and/or ablation should be further investigated, as the tests performed have shown promising results.

## REFERENCES

- [1] International standard, 2011, IEC 62271-200, *High voltage switchgear and controlgear - Part 200: AC metal-enclosed switchgear and controlgear for rated voltages above 1 kV and up to and including 52 kV. Annex AA: "Internal arc fault – Method to verify the internal arc classification (IAC)"*
- [2] K. Anantavanich et al., 2010, *Calculation of Pressure Rise in Electrical Installations due to Internal Arcs Considering SF6-Air Mixtures and Arc Energy Absorbers*, PhD Thesis (Publisher), Aachen, Germany.
- [3] D. Rochette et al., 2008 "Numerical Investigations on the Pressure Wave Absorption and the Gas Cooling Interacting in a Porous Filter, During an Internal arc Fault in a Medium-Voltage Cell," *Power Delivery, IEEE Transactions on*, vol.23, no.1, pp.203-212
- [4] T. Oyvang et al., 2011, "High Current Arc Erosion on Copper Electrodes in Air," *Electrical Contacts (Holm), 2011 IEEE 57th Holm Conference on*, vol., no., pp.43-48